International Journal for Housing Science and Its Applications
Publish August 3, 2025. Volume 46, Issue 3 Pages 548-557

https://doi.org/10.70517/ijhsa46339

Computational simulation study of arrangement optimization in the structural design of avalanche control fences from G218 Narathi to Baruntai

Jialun Zou[1,2] and Jian Liu[2,*]
[1] College of Transportation and Logistics Engineering, Xinjiang Agricultural University, Urumqi, Xinjiang, 830000, China
[2] The Xinjiang Communications Science Research Institute Co., Ltd., Urumqi, Xinjiang, 830000, China
Corresponding authors: (e-mail: 18943028620@163.com).

Abstract The G218 Narathi-Balentai highway is exposed to the impact risk of avalanche loading. This paper explores the constructional characteristics, column materials and structural design of the control fence of this section of highway, simulates avalanche based on RAMMS-AVALANCHE model, analyzes the force situation of the fence under the impact of avalanche with different parameters, and provides relevant countermeasures for the structural arrangement of the control fence. The avalanche dynamic process is simulated by the tanα parameter graphing method and the probabilistic relationship graph between avalanche throw and fall. The finite element analysis model of different types of fences is established to simulate the force state of fences when the height of avalanche impact is 1m, 2m and 3m. Under the consideration of different working conditions, the displacements and stresses of different types of fences were calculated, and the force characteristics of the fences were analyzed. By analyzing and demonstrating the force under avalanche load of three types of fences, the force characteristics of different forms of fences under avalanche load are obtained, and finally the diversion tip wedge structure is adopted to provide reference for similar disaster prevention projects.

Index Terms Avalanche control fence, RAMMS-AVALANCHE, tanα parameter graphing method, finite element analysis

I. Introduction

National Highway G218 is an extremely important provincial highway in Xinjiang Uygur Autonomous Region of China. The line connects the towns of Nalati and Baluntai, with a total length of 217.6 km.This road is a convenient channel connecting the Yili Valley region with Korla in the southern border, and plays a crucial role in the economic development of the Xinjiang Uygur Autonomous Region. However, the road section is characterized by steep mountains, cold weather, heavy snowfall, and frequent avalanche disasters, which seriously hinder the local economic development. According to statistics, dozens of major avalanches have affected the highway to varying degrees in recent years [1]. The G218 line is subject to the control of the westerly airflow and topographic conditions, with more snowfall weather in the winter half year, average temperature -15~-20℃, and the lowest temperature can reach -36℃ [2], [3]. The first snow appeared in early September, the final snow day in late April, special years in June also have snowfall days appear [4]. The average multi-year snow accumulation in the region is more than 50 cm, and the maximum snow depth can reach 150 cm. According to the local road snow damage weather station records, the accumulated snowfall in the region in the year of 2023-2024 reached more than 400 cm, which indicates that the snowfall and the resultant snow accumulation is fully reached the critical depth value of avalanches, which provides sufficient material security for avalanches [5].

Avalanche is not just a road disease, it has become a social hazard, in many countries of the world such as the former Soviet Union, Japan, the United States, Canada, Switzerland, Peru and other countries have avalanche disaster [6]. Many areas in China also suffer from the threat of avalanches, such as the southeastern part of the Tibetan Plateau, the southern edge of the Tibetan Plateau, the northern edge of the Tibetan Plateau, the Tianshan and Altay Mountains, the Greater and Lesser Xing'an Mountains, the Changbai Mountains, and the northeastern part of the Tibetan Plateau, where avalanches are a constant threat to the lives of the mountain inhabitants and the safety of their properties [7]-[9]. Avalanches can cause the collapse of houses, casualties, resulting in the death of cattle and sheep and other livestock have occurred repeatedly, the lives of herdsmen are also under constant threat, travelers, mountaineers are often killed by avalanches, and the increasingly fragile ecological environment is also continuously damaged by avalanches [10]-[13]. At present, the prevention and control of avalanches has become the urgent desire of all sectors of society.

The study uses the RAMMS-AVALANCHE model to simulate the 2011 avalanche event from G218 Narathi to Baruntai, and further compares and analyzes the RAMMS-AVALANCHE numerical simulation results of the avalanche throw with various theoretical calculations. The avalanche dynamics is investigated through the tanα parameter graphing method and the probabilistic relationship graph between avalanche throw and fall. Relying on the force characteristics of G218 highway project under the action of avalanche load, we establish finite element analysis models of different types of fences, analyze the force of fences under the action of avalanche impact with different parameters, and put forward the optimization strategy of the structural arrangement of prevention and control fences according to the analysis results.

II. Avalanche control fence structure design and arrangement requirements

II. A. Tectonic features

According to the G218 Narathi to Barendai highway design requirements of this site, this section of the line guardrail for reinforced concrete guardrail, which consists of columns, upper sill, lower sill, railing piece, post cap components, the use of prefabricated and field assembly process. The length of each unit (the distance between the center of two adjacent columns) is 3.00, 1.59, 1.15m, and the height of the protective fence is 1.8m and 2.2m. Ground longitudinal slope is less than 6 ° lot, the length of the guardrail unit 3m, 6 ~ 12 ° lot guardrail unit length of 1.59m, 12 ~ 36 ° slope lot guardrail unit length of 1.15m. Each component are used in C30 concrete prefabrication.

II. B. Column materials

In view of the sulfate corrosion problem in inland areas, a series of measures have been taken in engineering, such as improving the performance of concrete itself, applying protective layer on the surface, wrapping isolation and so on. Although these methods for anti-sulfate corrosion has a certain role, but there are some problems. Improve the performance of concrete itself shall be mixed with anti-sulfur components, high cost, economically undesirable. Surface coating protective layer must be carried out under certain conditions, the operation process is more complex. Parcel isolation method in the parcel layer and concrete affinity is poor, easy to peel off with concrete, high cost, replacement difficulties. As an excellent high-strength, corrosion-resistant, high-temperature-resistant composite fiber material, FRP has excellent environmental adaptability and high cost performance, and has been widely used in engineering [14]. The use of FRP materials to replace concrete for the protective fence of G218 Narathi to Balendai will be able to improve the status of concrete sulfate corrosion and guarantee the safety of the project structure.

II. C. Structural design and numerical calculations

Protective fence column design and existing columns with the same size of the rectangular tube, cross-section size 120mm × 120mm, thickness of 5mm. in order to improve the bending capacity of the column, in the rectangular tube in the direction of the vertical line to set up cross ribs, fence column structure design as shown in Figure 1.

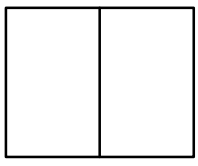

(a) Cross-section

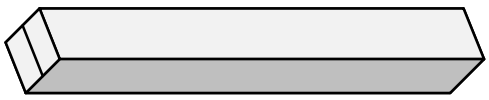

(b) The whole

Figure 1: Design of fence column structure

According to TB/T3522-2018 “Railway Line Protection Fence” on the fence design load, the man-made destructive force is taken as 1kN/m. The wind pressure is considered according to the wind class 11, and the standard value of the load is 0.6kPa. the seismic intensity is taken as 8 degrees [15]. According to the “Building Structure Design Code”, it is concluded that the combination design value of variable load effect control is the most unfavorable combination, in which the man-made incidental load is the main factor. The calculation model and load distribution of the fence are shown in Fig. 2.

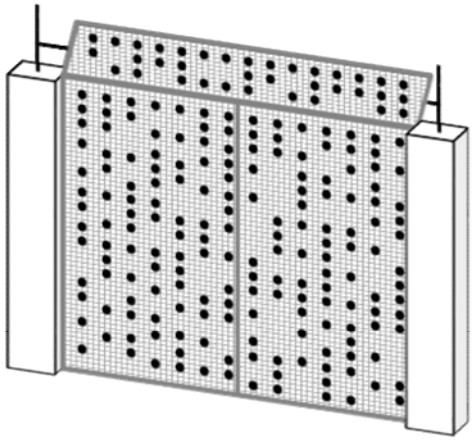

Figure 2: The fence calculation model and load distribution

For modeling analysis the columns are made of FRP and the metal mesh is made of Q345 steel, the material parameters are shown in Table 1. Because the wind load and man-made damage force under the action of the component to the main bending, so the bending strength to determine the plastic zone. The plastic zone numerical analysis is equivalent to the plastic zone of steel and concrete materials, FRP material into the plastic zone is considered as damage, while the steel into the plastic zone is only considered as yield.

Table 1: Material parameter

Material	Density/(10^3kg·m^{-3})	Elastic modulus/GPa	Poisson ratio
Glass steel	1.87	50.6	0.32
Q345 steel	7.69	206.3	0.24

As can be seen from the results of calculating the force on the FRP columns of the protective fence, the FRP columns are in good stress condition and no damage occurs. Among them, the maximum tensile stress of the column is 28.5MPa, and the maximum horizontal displacement is 61.7mm, which appears at the top of the column.

III. Avalanche simulation based on the RAMMS-AVALANCHE model

III. A. The RAMMS-AVALANCHE model

In this study, avalanche initiation, motion and stagnation processes in real complex terrain are simulated based on the RAMMS-AVALANCHE model with depth-averaged avalanche dynamics equations at its core [16]. After determining the key parameters such as avalanche fracture depth and friction coefficient, the validity of the simulation is evaluated by comparing the similarity between the actual field and the simulation results. The input parameters of the numerical simulation are adjusted according to the evaluation results, and finally credible numerical simulation results are obtained for the reconstruction of avalanche events.

The RAMMS-AVALANCHE model uses a Cartesian coordinate system to characterize the mean velocity U, and the relation for the mean velocity $U(x,y,t)$ is given below:

$$U(x,y,t)=\left[U_x(x,y,t)(x,y,t)^T\right] \tag{1}$$

$$n_a=\frac{1}{u}\left[U_x(x,y,t),U_y(x,y,t)\right]^T \tag{2}$$

Where: U_x is the value of the flow velocity in the X axis. U_y is the value of flow velocity in Y axis. T is the transpose of the mean flow velocity matrix. n_u denotes the direction of avalanche motion.

The RAMMS-AVALANCHE model was developed by coupling the VS model and the RKE model to ensure that the actual avalanche conditions are accurately reflected at both the macroscopic and granular levels. In the VS model, the friction coefficient is divided into two parts: the dry Coulomb friction coefficient μ, which is proportional to the normal stress N, and the turbulent friction coefficient ξ. The frictional resistance S is calculated by the following formula:

$$S = \mu N + \frac{\rho g u^2}{g}, N = \rho g h \cos\varphi \tag{3}$$

where: ρ is the density. g is the gravitational acceleration. φ is the angle of obliquity. h is the flow height. u is the vector $u = (u_x, u_y)^T$.

The VS model is jointly controlled by only two parameters, μ and ξ, which may not be able to capture the subtle variations due to the interactions between particles, clusters. Therefore the RKE model relates the friction coefficient to the random motion of the particles inside the avalanche by introducing the random kinetic energy R:

$$R(x, y, t) = \frac{1}{H}\int_0^H \hat{R}(x, y, z, t)dz \tag{4}$$

$$\mu(R) = \mu \exp(-\frac{R}{R_0}) \tag{5}$$

$$\xi(R) = \xi \exp(-\frac{R}{R_0}) \tag{6}$$

The relevant data to be entered into RAMMS-AVALANCHE are terrain data, start-up area information, friction information, forest cover area information, calculation parameters, orthophotos, etc. Among the key parameters are as follows:

(1) Avalanche Fracture Depth

Fracture depth refers to the average snow thickness of a certain thickness of snow layer in the avalanche initiation area that slides downward along the crack after the failure of a weak layer of snow that appears as a crack perpendicular to the slope surface under the action of gravity, temperature and other factors. To simplify the problem, the critical thickness of the snow layer on the slope, h_x, is used as the avalanche fracture depth:

$$h_k = \frac{c}{\rho(\sin\theta - \cos\theta \times \tan\varphi)} \tag{7}$$

where: c is the cohesion between the snow body and the slope. ρ is the density of snow (g·cm-3). θ is the slope angle of the hillside (°). φ is the angle of internal friction between snow and slope (°). $\tan\varphi$ is the coefficient of internal friction.

Where the snow accumulation characteristics study takes values as shown in Table 2. Snow accumulation characteristics such as cohesion, angle of internal friction and other snow accumulation characteristics are taken according to the field survey, the density is the actual measurement data on the site, and the slope and other topographic data are obtained from the DEM data analysis.

Table 2: Physical properties of snow

Snow type	Cohesion/(g·cm^{-2})	Coefficient of internal friction	Density/(g·cm^{-3})	Breaking strength/(g·cm^{-3})
Coarse snow	4	0.36	0.25	4.39

(2) Friction factor

The specific friction coefficient (μ, ξ) for the simulation is selected from the RAMMS friction coefficient reference table by combining the detailed parameters such as terrain characteristics, avalanche event recurrence period, avalanche cubic volume and altitude. The specific values are shown in Table 3.

Table 3: Reference table for RAMMS friction coefficients

Topographic feature	Elevation/m	The avalanche is reproducing	μ	ξ
Ditch landform	>1500	In 2011	1200	0.32

III. B. Calculation method of avalanche throw in relation to terrain

In order to reduce the interference caused by the complexity and randomness of avalanche disaster, the avalanche throwing range is often calculated by simplified models or empirical statistical formulas, and the mainstream

methods at present are the tanα mapping method, double inclination mapping method and avalanche arrival probability distribution map method. The double inclination method ignores the area of the avalanche initiation area, and instead considers the relationship between the average slope of the whole avalanche area (α angle) and the slopes of the avalanche initiation area and the movement area (β angle). The avalanche arrival probability distribution map, on the other hand, only considers the horizontal-vertical projection of the avalanche path by plotting the histogram of the L/H probability of avalanche throw-to-fall ratios and plotting their cumulative probabilities. In addition, the equivalent friction law from the geohazard discipline proposes a new parameter “avalanche kinematic eigenvalue” to construct a linear regression relationship based on the throw L, the vertical drop H, and the activation area S. The model is based on the relationship between the avalanche path, the vertical drop H, and the activation area S, which are the same as the avalanche path. In addition to the above simplified models and empirical statistical methods, avalanche throws can be obtained by reconstructing the avalanche event to simulate the entire avalanche motion with the help of numerical simulation software such as the RAMMS-AVALANCHE model. These methods are not only widely used in avalanche risk assessment, but also play an important role in road alignment, engineering design and transportation infrastructure maintenance.

IV. Computational simulation of avalanche power processes

IV. A. Statistical method of avalanche movement pattern data

Usually, empirical statistical formulas or simplified models can help to quickly grasp the laws of avalanche movement for disaster prevention and control. As the primary parameter to characterize the destructiveness of avalanche disaster, a lot of statistical analysis or probability distribution studies have been carried out at home and abroad, such as the relationship between the avalanche throw distance and parameters such as elevation difference, area of formation area, avalanche volume, pitch angle of the end point of the throw, and friction coefficient of the undercushion surface. The Design and Construction of Avalanche Protection Facilities: CH 517-80 adopts the tanα parameter mapping method to estimate the avalanche throw distance according to the terrain conditions. α is the inclination angle connecting the avalanche starting point A and termination point C, and it can be estimated by the friction angle between the snow and the ground. The method is to make a straight line with slope tanα from the avalanche starting point, and the intersection point with the longitudinal profile curve of the ground is the avalanche termination point, and the tanα parameter mapping method is shown in Fig. 3.

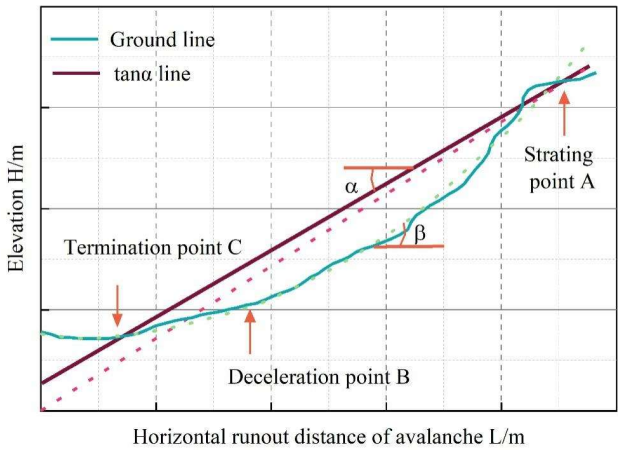

Figure 3: Plotting method with tanα

In Europe and the United States, the statistical method of double dip (α and β) is used to estimate the avalanche throw, and β is the average slope between the avalanche initiation point A and the deceleration point B. The empirical formulas for avalanche zones with different terrain features may be different, e.g., Norway $\alpha = 0.96\beta - 1.7°$. In Japan, by counting 603 surface avalanches and 155 full avalanches, the probabilistic relationship between the avalanche throw range L and the fall distance H was plotted as shown in Fig. 4. Measuring the values of L and H at any point on the avalanche throw line from the map, the avalanche arrival probability Q at that point can be found from the L/H ratio.

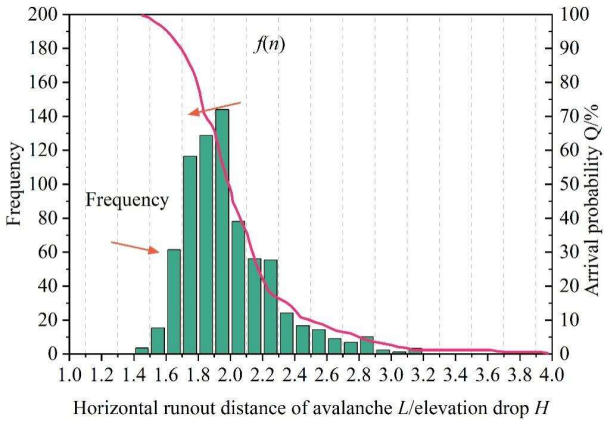

Figure 4: Avalanche arrival probability graph

The relationship between avalanche throw $L_{\max}$ and the area of avalanche formation zone S_{area} and the maximum height difference of avalanche $H_{\max}$ are estimated based on the equivalent friction coefficient for 36 medium-sized gouge-type wet snow avalanches on the G218 Nalati-Baruntai Highway, which can be used to determine whether the avalanche throw threatens the safety of the road or not.

The Coulomb friction model provides predictions of avalanche flow rates and impact distances in most cases, and is therefore often used in the estimation of macroscopic avalanche dynamics. Considering the presence or absence of basal friction, the upper and lower theoretical values of maximum flow velocity can be estimated, and the maximum avalanche frontal velocity varies as the square root of the total drop H, i.e., $v_{\max} \propto \sqrt{H}$. The overall force analysis of the hillside snow, if the whole layer of the hillside snow is considered to be broken, the critical snow thickness for avalanches to occur is:

$$h_k = \frac{c}{\rho(\sin\theta - \mu\cos\theta)} \tag{8}$$

where ρ is the density of snow, c is the cohesion between snow and hillside, μ is the coefficient of internal friction, and θ is the slope gradient of the hillside, the critical depth of snow increases as the slope gradient of the hillside decreases. The density of snow varies with snow age, and the rate of densification of fresh dry snow with intact crystalline form is maximum in the first 3 days after landing. The velocity v of avalanche body movement and the impact force F of avalanche on the facility surface can be estimated as respectively:

$$v = \sqrt{2g(h - \frac{Hl}{L})} \tag{9}$$

$$F = \frac{\rho v^2}{g}\sin^2\phi \tag{10}$$

where g is the gravitational acceleration, h and l are the height difference and horizontal projection length from the avalanche initiation point to the calculation point, respectively, and ϕ is the angle between the avalanche movement direction and the facility surface. Macroscopic empirical avalanche formulas generally have the limitation of a specific scope of application, and cannot take into account the entrainment effect, rheological modeling, particle rearrangement and agglomeration, and other fine-scale mechanical behaviors of avalanche flow. Studies have shown that the mass before and after an avalanche may increase by a factor of 4 on average, which is mainly affected by the plowing-type entrainment effect of avalanche fronts.

IV. B. Avalanche dynamics process simulation methods

The rapid motion and large deformation of snow are mainly controlled by particle rearrangement, and momentum transfer occurs by breaking inter-particle cohesion and creating new contacts. The special crystalline structure of snow grains results in a very complex and difficult to characterize inter-particle force chain. Discrete element method (DEM) is often used to capture the structural features of snow grains at the microfine scale, such as the non-homogeneous microstructure of snow grains based on microlamellar imaging, the phenomenon of snow grain agglomeration and coarse-graining, and the theory of fractal crystal fragmentation in wind-blown snow. The contact,

friction and fracture mechanical behaviors between snow grains can be captured by defining the connecting bonds for force conduction between snow grains, which can be used for the simulation of avalanche dynamic processes, such as the loading fracture and crack extension behaviors of the soft snow layer in slab avalanches, and the estimation of impact pressure by avalanche-obstacle interactions.

In this paper, based on a porous viscoelastic-plastic model considering snow-hardening characteristics, four avalanche flow types in the GEODAR dataset are simulated using the material point method, and it is verified that the two highly shear flows, cold dense avalanches and warm shear avalanches, are similar to the non-viscous particles flow, and the latter two flow types, i.e., the warm plugging avalanches and the sliding plate avalanches, occur when the adhesion force between snow particles is dominant.

The results of the study show that cold dense type avalanches, which are non-viscous dense flow avalanches, have the furthest impact distances and the largest flow velocities, and the relationships between the normalized maximum flow velocity, deposition height and Mβ are shown in Fig. 5. Usually, avalanche hazard zoning and mapping pay most attention to this type of avalanche. The flow process of this type of avalanche is mainly affected by the friction of the substrate rather than the characteristics of the snowpack, so theoretically, the rheological model of granular flow can be used to study the dynamics of cold dense avalanches. The material point method can easily deal with complex boundaries and is used to simulate avalanche dynamics in three-dimensional complex terrain. The material point method naturally ensures the conservation of mass and momentum, but the fixed mass also leads to the difficulty of adding or removing particles in the system, so special treatment is needed when considering the change of avalanche entrained mass.

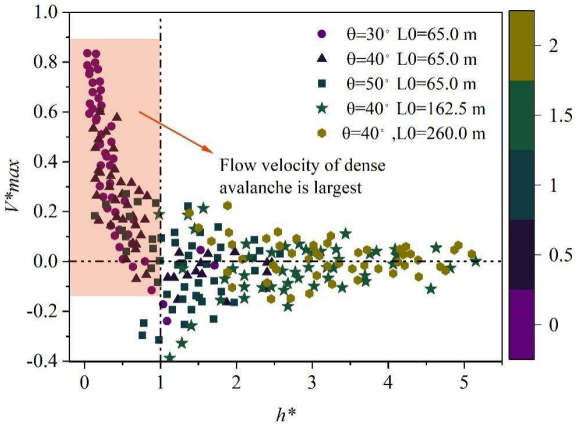

Figure 5: Relationship between max flow velocity, deposition height and Mβ

IV. C. Results of the mechanical analysis of the avalanche control fence

IV. C. 1) Formulation of avalanche impact pressure values

The values of avalanche body pressure at the corresponding fences at different sections of the G218 highway project are shown in Table 4.V1, V2, P1, P2, and P3 denote the end velocity of the avalanche body obtained from the theoretical formula, the end velocity of the avalanche from the avalanche special guideline, the pressure obtained from the theoretical formula, the pressure value of the avalanche special guideline, and the pressure after the avalanche special guideline after the protection, respectively. In the case of no protection, the avalanche generated pressure is larger. The avalanche special guidance proposal also gives the avalanche protection engineering measures on the slope path where avalanches may occur, using the dual measures of snow blocking fence and diversion wedge to prevent avalanches from hitting and damaging the fence. After the protection, the pressure of avalanche loads at the fence is greatly reduced. According to the corresponding values of avalanche body pressure at the fence in different sections, the protection program of “snow blocking fence + sharp wedge” is adopted in 1~6 and 9 sections. Sections 7, 8, 16, 17 and 18 adopt the protection scheme of “snow blocking fence + sharp wedge + energy dissipation pool”. Sections 11, 12, 13, 14 and 15 are protected by a “spiked wedge + snow fence”. Section 10 is protected by a “spiked wedge”.

Table 4: The pressure value of the avalanche in different sections of the bridge

N	Slope length/m	Mean grade/°	V1 (m/s)	V2 (m/s)	P1/kPa	P2/kPa	P3/kPa
1	301.89	25.46	26.56	26.47	281.65	282.19	47.27
2	181.27	32.85	28.25	27.66	320.24	308.71	51.87
3	212.49	35.38	30.51	28.48	376.61	318.2	53.29
4	262.61	32.85	30.6	27.74	371.78	309.78	51.88
5	200.23	33.99	29.7	28.15	349.95	313.67	52.6
6	141.44	33.83	27.13	27.93	351.94	373.47	52.11
7	249.7	27.01	26.91	26.73	343.96	345.85	56.51
8	297.43	22.79	24.6	26.07	290.08	325.97	52.95
9	193.55	27.81	25.86	26.82	322.13	348.5	56.78
10	160.36	36.43	29.11	28.38	405.82	384.16	62.53
11	125.11	37.83	27.72	28.41	369.03	388.1	63.1
12	100.72	44.76	28.05	29.44	382.54	413.26	67.38
13	180.99	30.06	26.85	27.33	343.05	357.63	58.35
14	173.75	29.53	26.39	27.39	332.38	356.2	57.92
15	174.16	37.93	30.46	28.69	445.59	390.78	63.56
16	151.02	27.13	24.09	26.72	278.15	343.16	56.13
17	168.15	28.8	25.73	27.21	315.61	351.9	57.37
18	103.06	34.38	24.8	27.65	293.69	370.43	60.31

IV. C. 2) Calculation of loads and determination of the structural form of the fence

G218 highway project superstructure mainly adopts 20m, 30m span assembled T-beam, and the substructure is dominated by double-post fence, gantry fence and T-shaped fence. In this paper, the above three types of fences for avalanche load calculation. Since most of the fences in the project are about 20m high, the height of the fences is taken as 20 m. The avalanche pressure value is taken as the maximum pressure value of 67.3kPa after protection, and different avalanche impact head heights are considered for analysis. The structural dimensions of different types of fences are shown in Table 5. The structural forms of the fence include single-width double-post fence (Type 1), single-width T-shaped fence (Type 2), whole-width gantry fence (Type 3), and whole-width gantry fence (with tie beams) (Type 4).

Table 5: Different types of bridge structure size

Fence type	Height/m	Rectangular fence	Socket	Girder
Type 1	20	1.8	-	1.4×1.2
Type 2	20	3.2×2.2	7.4×7.4	-
Type 3	20	2.6×2.8	3.4×8	-
Type 4	20	2.6×2.8	3.4×8	1.6×1.6

IV. C. 3) Analysis of calculation results

MIDAS software is used to establish the finite element analysis model of different types of fences, and simulate the force state of the fence when the height of avalanche impact is 1m, 2m and 3m, and the displacement of the top of the fence, the maximum stress of the bottom of the fence, and the maximum stress of the pile foundation of the different forms of fences under the impact of the avalanche pressure of 67.3kPa are shown in Table 6. The form of substructure contains single width double column fence + pile foundation (S1), single width T-shaped fence + group piles (S2), the whole width of the gantry fence + group piles (S3), the whole width of the gantry fence + sill tie beam + group piles (S4).

Table 6 shows that when the avalanche impact pressure is certain, with the increase of the avalanche impact height, the top displacement of the fence, the maximum stress of the fence body and the maximum stress of the pile foundation are all increasing linearly. For the single double-post fence (S1), in the avalanche impact height of 1m, the maximum stress of the pile foundation is 2.1MPa, less than the tensile strength of the fence (2.2MPa), it can be considered that at this time the double-post fence is still in the elastic working state. When the avalanche impact height of 2m, the maximum stress of the pile base is 4.6MPa, has been greater than the tensile strength of the fence (2.2MPa), it can be considered that at this time the double-post fence pile base has been in the failure state. Therefore, for this project 20m fence height double post fence, in the avalanche scour height of 1m range,

double post fence force to meet the design requirements. When the avalanche scouring height exceeds 1m, or the avalanche pressure value exceeds 67.3kPa, it is necessary to consider increasing the protective measures to avoid the fence cracks and plastic damage.

For the whole width of the gantry fence (S3), when the avalanche impact height is 1m, the maximum stress at the pile foundation is 1.4MPa, which is smaller than that of the single width double-post fence (S1) under the same working condition (2.1MPa). The maximum stress at the bottom of the fence is 1.3 MPa, which is larger than the maximum stress value (0.4 MPa) of the single-width double-post fence under the same working condition. This is because the gantry fence adopts the form of bearing+double pile foundation, and the two pile foundations share the avalanche load, so the stress generated by each pile foundation is smaller than that of the double-post fence. The stress of the fence is larger than that of the double-post fence, which is due to the larger spacing of the gantry fence, the lack of effective contact at the top of the piles, the lower stiffness of the fence columns on one side, the strain is larger, so the stress suffered is larger, and the deformation is also larger. But in this case, the gantry fence are in the elastic working range. In the avalanche impact height of 2m, the fence bottom maximum stress of 2.6MPa, more than the tensile strength of the fence (2.2MPa), it can be considered that at this time the fence has produced cracks in the plastic working state, this time we should consider increasing protective measures to avoid the fence cracks and plastic damage.

For T-shaped fence (S2), in the avalanche impact height of 1m, the maximum stress at the pile base is 2.4MPa, which is comparable to the maximum stress value of 2.1MPa for single-width double-post fence. But the maximum stress at the bottom of the fence is 0. This is because the fence body above the bearing platform of the T-shaped fence is not constrained, and the degree of freedom is larger, so it does not produce strain under the action of the load.The stress at the pile base of the T-shaped fence is the largest of the above three forms of fences, which is due to the avalanche load is mainly borne by the strain produced by the pile base of the T-shaped fence. When the avalanche impact height of 2m, the maximum stress of the pile base is 4.2MPa, more than the tensile strength value of the fence (2.2MPa), it can be considered that at this time the pile base has produced cracks, in the plastic working state, it is necessary to consider the increase of protective measures, so as to avoid cracks in the fence as well as plastic damage.

In summary, this project can be used to divert the pointed wedge, in order to ensure that the fence is in the elastic working state.

Table 6: Stress under avalanche shock

Substructure	1m			2m			3m		
	Top shift/mm	Maximum stress at the bottom/MPa	Maximum stress of pile/MPa	Top shift/mm	Maximum stress at the bottom/MPa	Maximum stress of pile/MPa	Top shift/mm	Maximum stress at the bottom/MPa	Maximum stress of pile/MPa
S1	11.8	0.4	2.1	23.1	0.5	4.6	35.1	0.7	11.8
S2	11.93	0	2.4	24.73	0	4.2	36.4	0	11.93
S3	22.8	1.3	1.4	43.3	2.6	2.3	65.8	4.2	22.8
S4	10.5	0.3	0.9	17.16	0.1	1.2	26.6	1.6	10.5

V. Conclusion

This study relies on the G218 Narathi-Balentai highway project, and the following conclusions are obtained through the RAMMS-AVALANCHE model to study the force state of the project under avalanche loading:

When the avalanche pressure value does not exceed 67.3kPa and the avalanche impact height is within 1m, the double-post fence, gantry fence, and T-shaped fence are in elastic working state, and the structure is in a safe state. When the avalanche pressure value of 67.3kPa and avalanche impact height of more than 1m, 3 types of fence are pier or pile concrete cracking, this fence is in the plastic working state, the deformation is irreversible, it can be considered at this time fence concrete failure, the need to increase protective measures. This project adopts shunt tip wedge to ensure that the fence is in the elastic working state.

Funding

The Third Xinjiang Scientific Expedition Program (2022xjkk0602).

References

[1] Yiwei, T. A. O., Fanghua, Z. H. A. N. G., Bixin, Y. U., Anbei, L. I., Yi, H. U., & Dan, W. A. N. G. (2024). Analysis of the causes and forecast of the extremely heavy snowfall in Altay Area that triggered avalanches in January 2024. Torrential Rain and Disasters, 43(4), 407-418.

[2] Liu, J., Sun, X., Guo, Q., Yang, Z., Wang, B., Yao, S., ... & Hu, C. (2024). Snow Avalanche Susceptibility Mapping of Transportation Corridors Based on Coupled Certainty Factor and Geodetector Models. Atmosphere, 15(9), 1096.
[3] Yang, J., Li, L., & Liu, Y. (2024). Dynamic spatiotemporal quantification of avalanches in the Central Tianshan Mountains by integrating air–space–ground collaborative sensing and snow field–terrain filters. International Journal of Digital Earth, 17(1), 2432525.
[4] SHU, X., WU, X., WEN, H., LING, S., & SONG, D. (2023). Comparison of snow avalanche susceptibility assessment and potential snow avalanche release areas identification along Yining-Aksu railway, Xinjiang Tianshan Mountains. Journal of Engineering Geology, 31(4), 1200-1212.
[5] Hao, J. S., Huang, F. R., Liu, Y., Amobichukwu, C. A., & Li, L. H. (2018). Avalanche activity and characteristics of its triggering factors in the western Tianshan Mountains, China. Journal of Mountain Science, 15(7), 1397-1411.
[6] Statham, G., Haegeli, P., Greene, E., Birkeland, K., Israelson, C., Tremper, B., ... & Kelly, J. (2018). A conceptual model of avalanche hazard. Natural hazards, 90, 663-691.
[7] Liu, J., Zhang, T., Hu, C., Wang, B., Yang, Z., Sun, X., & Yao, S. (2023). A study on avalanche-triggering factors and activity characteristics in Aerxiangou, West Tianshan Mountains, China. Atmosphere, 14(9), 1439.
[8] Wang, Y. F., Cheng, Q. G., Lin, Q. W., Li, K., & Yang, H. F. (2018). Insights into the kinematics and dynamics of the Luanshibao rock avalanche (Tibetan Plateau, China) based on its complex surface landforms. Geomorphology, 317, 170-183.
[9] Chu, D., Liu, L., Wang, Z., Nie, Y., & Zhang, Y. (2024). Snow Avalanche Hazards and Avalanche-Prone Area Mapping in Tibet. Geosciences (2076-3263), 14(12).
[10] Schweizer, J., Mitterer, C., Techel, F., Stoffel, A., & Reuter, B. (2020). On the relation between avalanche occurrence and avalanche danger level. The Cryosphere, 14(2), 737-750.
[11] Gruber, U., & Bartelt, P. (2007). Snow avalanche hazard modelling of large areas using shallow water numerical methods and GIS. Environmental Modelling & Software, 22(10), 1472-1481.
[12] Strapazzon, G., Schweizer, J., Chiambretti, I., Brodmann Maeder, M., Brugger, H., & Zafren, K. (2021). Effects of climate change on avalanche accidents and survival. Frontiers in physiology, 12, 639433.
[13] Thakuri, S., Chauhan, R., & Baskota, P. (2020). Glacial hazards and avalanches in high mountains of Nepal Himalaya. Nepal Mountain Academy, 87, 1075.
[14] Agarwal Pankaj,Kumar Mukesh,Sharma Ankush,Choudhary Mahavir,Shekhawat Deepika & Patnaik Amar. (2022). Experimental and numerical investigation on slurry erosion performance of hybrid glass/steel fiber reinforced polymer composites for marine applications. Polymer Composites,43(8),5592-5610.
[15] Long Shi,Dongyuan Wang,Kai Cui & Chunxiao Xue. (2021). Comparative evaluation of concrete sand-control fences used for railway protection in strong wind areas. Railway Engineering Science,29(2),1-16.
[16] T. Sardar,Aigong Xu & A. Raziq. (2017). Snow Avalanche Susceptibility Based Assessment of Release Zones over Complex Terrain of Siachen Glacier Applying Ramms and Dsr as Active Macroclimatic Factor. Procedia Computer Science,107,427-435.